Am J Physiol Endocrinol Metab 288: E948–E956, 2005.
First published December 29, 2004; doi:10.1152/ajpendo.00216.2004.

Biophysical evidence that connexin-36 forms functional gap junction channels between pancreatic mouse β-cells

Alonso P. Moreno,[1] Viviana M. Berthoud,[2] Gregorio Pérez-Palacios,[3] and E. Martha Pérez-Armendariz[3]

[1]*Krannert Institute of Cardiology, Indiana School of Medicine, Indianapolis, Indiana;* [2]*Section of Hematology/Oncology, Department of Pediatrics, University of Chicago, Chicago, Illinois; and* [3]*Facultad de Medicina, Departmento de Medicina Experimental, Unidad de Investigación, Enseñanza y Comunicación Ensalud Sexual y Reproductiva, Universidad Nacional Autónoma de México, Mexico City, Mexico*

Submitted 25 May 2004; accepted in final form 15 December 2004

Moreno, Alonso P., Viviana M. Berthoud, Gregorio Pérez-Palacios, and E. Martha Pérez-Armendariz. Biophysical evidence that connexin-36 forms functional gap junction channels between pancreatic mouse β-cells. *Am J Physiol Endocrinol Metab* 288: E948–E956, 2005. First published December 29, 2004; doi:10.1152/ajpendo.00216.2004—Connexin-36 (Cx36) is the only gap junction protein that has been unambiguously identified in rodent pancreatic β-cells. However, properties of gap junction channel unitary currents between β-cells remain unrevealed. To address whether Cx36 forms functional channels in β-cells, we characterized biophysical properties of macro- and microscopic junctional currents recorded from dual whole cell voltage clamp isolated pairs of dispersed mouse β-cells. Electrical coupling was recorded in 80% of cell pairs with a junctional conductance (g_j) of 355 ± 45 pS (n = 20). Transjunctional voltage dependence was identified in three of seven cell pairs with high-input membrane resistances. Normalized steady-state g_j (G_j) and transjunctional-voltage relation were well described by a two-state Boltzmann equation [maximal conductance (G_{max}) = 1.0, voltage-insensitive conductance (G_{min}) = 0.3 and 0.28, voltage gating sensitivity (A) = 0.21 and 0.23, and voltage at which one-half of the initial voltage-dependent conductance was reached (V_o) = −85 and 87 mV for negative and positive potentials, respectively]. Halothane reversibly uncoupled β-cell pairs, and, during recovery, unitary conductances of 5–10 pS were recorded while using patch pipettes containing mainly CsCl. Although these properties are similar to those previously described for Cx36 channels in mammalian cell systems, we found that β-cell junctional currents were insensitive to quinine. Cx36 transcript and protein expression in islets and freshly dispersed cell preparations was confirmed by RT-PCR and immunofluorescence. In conclusion, biophysical properties of junctional channels between β-cells are similar but not identical to those previously described for homomeric Cx36 channels. Cell type-specific mechanisms that may account for these differences are discussed.

islets of Langerhans; insulin; connexin; intercellular communication

CONNEXINS CONSTITUTE A FAMILY of homologous transmembrane proteins that form gap junction channels that allow direct traffic of ions and cytoplasmic molecules between adjacent cells. Direct intercellular communication has been found necessary to maintain tissue homeostasis, and some connexin mutations have been clearly related to human diseases (16, 52).

The islet of Langerhans is considered to be the fundamental functional unit for insulin secretion and glucose homeostasis. β-Cells secrete insulin and constitute ~80% of the mouse islet of Langerhans inner mass. They are surrounded by three other types of endocrine cells localized at the periphery of the islet: α-cells, which produce glucagon, δ-cells, which secrete somatostatin, and PP cells, which produce pancreatic polypeptides. Gap junctions (25) and electrical coupling (11) have been demonstrated between mouse islet β-cells. When glucose changes within a physiological range (5–36 mM), it induces synchronous oscillations in different cell parameters that occur in phase within a single mouse islet; these include intracellular electrical activity (26), interstitial potassium concentration (33, 32), interstitial calcium concentration (31), intracellular calcium concentration (39), and insulin secretion (38), which may be coordinated by gap junctions.

In a previous study, we characterized the biophysical properties of gap junctional conductance (g_j) recorded in isolated pairs of freshly dissociated mouse β-cells under dual whole cell voltage-clamp conditions (35). Dye coupling with Lucifer yellow (LY) was not detected between cell pairs. In contrast, a high percentage of the cell pairs studied (~70%) were found to be electrically coupled with a g_j of 215 ± 110 (SE) pS, which was not voltage sensitive. Although it was expected that this small g_j would be provided by a few gap junction channels with unitary conductances similar to those characterized at that time in other tissues (50–120 pS), no single gap junction channel currents larger than the noise limit resolution (20 pS) were recorded during uncoupling induced by 2 mM octanol. To explain those results, we had proposed that either the unitary conductance of a single gap junction channel (γ_j) between β-cell pairs is <20 pS or intercellular channels between β-cells gate with distinct kinetics than those recorded between cell pairs isolated from other tissues. At that time, connexin-43 (Cx43) was the only connexin identified in rat islet cells by imunofluorescence and RT-PCR studies (23, 24; see also below). However, Cx43 channels in native (8, 34) and mammalian cell expression systems (29) were known to be voltage dependent and permeable to LY and had a main γ_j of 110 pS. Thus we proposed that gap junction channels in mouse β-cells might express a different connexin than Cx43 (32, 35).

In agreement with this hypothesis, and after several other connexins had been cloned during the past 10 years, molecular studies have identified two other connexins in rodent islet cell preparations [Cx45 (9) and Cx36 (40)]. In β-cells, reports on the expression of Cx43 and Cx45 have been controversial. Although Cx43 and Cx45 transcripts have been identified in fluorescence-activated cell sorter purified rat β-cells and total

Address for reprint requests and other correspondence: E. M. Pérez-Armendariz, UNISSER, Departamento de Medicina Experimental, Facultad de Medicina, UNAM, Hospital General de México, Dr. Balmis no. 148, Colonia Doctores México, D.F., 06726, México (E-mail: eperez@servidor.unam.mx).

The costs of publication of this article were defrayed in part by the payment of page charges. The article must therefore be hereby marked "*advertisement*" in accordance with 18 U.S.C. Section 1734 solely to indicate this fact.

mouse pancreas by RT-PCR (9), their protein expression in β-cells has not been demonstrated. In addition, as for Cx43 (see above), no evidence has been found for the expression of characteristic Cx45 homomeric unitary currents (28, 48) in g_j recordings from mouse β-cell pairs (35). Recently, transcription of Cx43 and connexin-45 (Cx45) was found to be restricted to the vascular compartment of the islets using different types of mice with connexins embedded with LacZ reporter genes. Nonetheless, it remains to be investigated whether these findings reflect a limitation in the sensitivity of the reporter gene analysis resulting from very low levels of transcription of Cx43 and/or Cx45 in β-cells or the actual absence of expression of these connexins in this cell type (47).

In contrast, Cx36 transcript and protein have been clearly documented in rat (20, 40) and mouse (40) islets. In addition, transcription of Cx36 has been localized to β-cells in Cx36-LacZ embedded transgenic mice (47). Moreover, a correlation between insulin content and Cx36 expression (22) as well as modulation of insulin content induced by Cx36 (20) have been found. Therefore, at the present time, Cx36 is considered to be the major connexin expressed in β-cells. However, it remains to be demonstrated if Cx36 forms functional channels in native rodent β-cells. In the present work, we address this issue by further characterizing the biophysical properties of g_j recorded from dual voltage-clamp freshly dispersed mouse β-cell pairs in recordings with a higher signal-to-noise ratio. These properties are compared with those described for Cx36 channels recorded from mammalian cell expression systems (1, 44, 46). Our results show that the biophysical properties of gap junction channels from mouse β-cells are similar, but not identical, to those recorded from Cx36 channels in cell expression systems. Cell mechanisms that may account for these differences are discussed.

METHODS

Pancreatic β-Cell Cultures

β-Cell cultures were obtained by isolating CD1 mouse islets and dissociating them as previously described (35). Cells were cultured for 8–12 h in RPMI medium supplemented with 16 mM glucose, 10% FBS, 100 U/ml penicillin, and 100 μg/ml streptomycin (GIBCO Laboratories) and were maintained in a 5% CO_2-95% air incubator at 37°C for 6–9 h before electrophysiological recordings and immunofluorescence studies.

Identification of Pancreatic β-Cells

Pancreatic sections and islet cells cultured for 8–12 h were fixed in 70% ethanol at −20°C for 20 min. After their preincubation in 2% albumin Krebs Ringer saline (KRS) solution, pH 7.4, tissue sections and cell cultures were incubated for 2 h with a specific guinea pig antiserum against porcine insulin previously characterized (50) at a dilution of 1:2,000. After several rinses, insulin-positive cells were revealed by their incubation for 2 h with FITC-conjugated secondary antibodies against guinea pig IgG used at a dilution of 1:100. To estimate the fraction of β-cells, monochromatic digitized images of three fields of islet cells cultured for 8 h ($n = 3$ cell cultures) selected at random were acquired at both phase-contrast and fluorescence microscopy at ×10 magnification. Images were analyzed for the fraction of insulin-positive cells. To test for specificity of the anti-insulin antibody, pancreatic sections with endocrine and exocrine acinar tissue were used as positive and negative controls, respectively. In addition, fibroblasts were used as internal cell controls in islet cell cultures grown for 36 h.

Identification of Cx36

Immunofluorescence studies. Cells were fixed in 70% ethanol at −20°C for 20 min. After their preincubation in 2% albumin in KRS, cells were incubated for 2 h with a specific affinity-purified polyclonal antibody against a peptide of the carboxyl terminus of rat and mouse Cx36 (37) at a 1:100 dilution. After several rinses, cells were exposed to rhodamine-conjugated goat anti-rabbit IgG antibodies. For double-labeling experiments, after cells were exposed for 2 h to anti-porcine insulin antibodies and rinsed, they were incubated for 2 h with anti-Cx36 antibodies. Binding of primary antibodies were revealed with FITC- and rhodamine-conjugated secondary antibodies. The same field of the section was analyzed sequentially under FITC and rhodamine excitation filters. Monochromatic fluorescence-digitized images at each excitation wavelength were acquired using a Hamamatsu digital camera (ORCA) and Metamorph software (Universal Imaging, West Chester, PA). Images were pseudocolored and color encoded to analyze for colocalization of both signals (data not shown). To test for specificity of labeling for Cx36, the olfactory bulb and the islet of Langerhans were used as positive control tissues. Exocrine acinar cells from pancreatic sections were used as a negative control.

RT-PCR studies. Islets and olfactory bulb were homogenized in TRIzol-guanidinium thiocyanate, and RNA was isolated according to the protocol provided by the manufacturer (Life Technologies, Gaithersburg, MD). Denatured total RNA (1 μg) was subjected to cDNA synthesis using the Superscript One Step RT-PCR kit system (Invitrogen). *Taq* polymerase, $MgCl_2$, and KCl buffer concentrations were used following the manufacturer's directions. Oligonucleotide primers (Life Technologies) were used at 200 ng in a 50-μl final volume reaction. The Cx36 oligonucleotides used were as follows: 5′-TGCAGCAGCACTCCAC TAGATTG(44–67), 5′-GTCTCCTTACTGGTGGTCTCTGTG (491–468), and 5′-CATAGGCAGAGTCACTGGACTGAG (961–938), as previously designed by Guldenagel et al. (15, 42). The protocol used included a predenaturation step at 90°C for 2 min followed by a 55° C step for 35 min to generate cDNA. PCR was carried out for 40 cycles using a thermal cycler as follows: denaturing at 94°C for 15 s, annealing at 58°C for 30 s, and elongation at 72°C for 1 min. For final extension, a 10-min step at 72°C was used. RT-PCR products were separated in 1.5% agarose gel and visualized with ethidium bromide. A low DNA mass ladder was used as standard marker (Life Technologies). Control experiments included amplifications from RNA samples incubated in the presence of DNase I to control for contamination of residual DNA (15). Negative controls included reactions performed in the absence of RT before PCR amplification and some in which water was added instead of RNA. Controls also included detection of β-actin transcript using specific oligonucleotides (15, 36), the amplicon mass of which differs from the one amplified from genomic DNA, performed in parallel to detection of Cx36 transcript.

Electrophysiology

Junctional conductance. Electrophysiological recordings of junctional (I_j) and nonjunctional (I_{nj}) currents were carried out using the dual whole cell voltage-clamp technique (Dual EPC-9; HEKA Elektronik, Lambrecht/Pfalz, Germany). Junctional currents (I_j) for each cell pair were recorded during a "slow-frequency" pulse protocol where hyperpolarizing 5-mV voltage steps of 300 ms were applied alternatively to each one of the cells in a pair at 0.5 Hz. Along this protocol, the membrane potential of both cells was maintained at 0 mV. The g_j was calculated after dividing the I_j recorded in the nonpulsed cell of the pair by the voltage applied to the pulsed one. Patch pipettes were filled with a solution containing (in mM) 130 CsCl, 0.5 $CaCl_2$, 10 HEPES, 10 EGTA, and 3 Mg^{2+}-ATP at pH 7.2. During recording, cells were kept at room temperature in a cesium-containing solution (160 mM NaCl, 7 mM CsCl, 2.0 mM $CaCl_2$, 0.6 mM $MgCl_2$, 5.0 mM $CdCl_2$, 5 μM TTX, 5.0 mM $BaCl_2$, and 10 mM

HEPES, at pH 7.4). Cultured β-cells remained round between 6 and 9 h of plating. Cell pairs recorded were of a macroscopic similar size. Slight cell size differences were compensated automatically by the electronic adjustment of the capacitance circuit in both amplifiers. Electrodes of 3–5 MΩ before sealing and patch break were used to reduce the interference of electrode resistance during gating. Series resistance was electronically compensated up to 69% to eliminate the voltage drop across the measuring electrodes and compensate equally well for the junctional resistance than for the resistance of other membrane channels (HEKA Elektronik). Data were simultaneously digitized for recording on VCR tapes (Neurocorder 840; Neurodata Instruments, New York, NY) and into a computer through the EPC9 AD/DA hardware system (HEKA). Traces were digitized at 11 kHz and acquired at 1 kHz for analysis.

Transjunctional voltage dependence. Transjunctional voltage dependence of junctional channels was determined through the application of a series of voltage ramps to one cell while recording the corresponding I_j in the other cell of the pair. The g_j was calculated by dividing the I_j obtained during the voltage ramp by the voltage ramp values. Ramps had durations of 50 and 100 s with a slope of 0.5–1 mV/s and were applied through HEKA software. The resulting conductance was plotted against the applied transjunctional voltage. Voltage gating parameters were determined after fitting the conductance curve to a single Boltzmann relation using Origin software (Microcal Software, Northampton, MA). These parameters included the voltage at which half of the initial voltage-dependent conductance was reached (V_o), voltage-insensitive conductance (G_{min}), maximal conductance (G_{max}), and voltage gating sensitivity (A).

Single channels. Single channel conductance was obtained during long voltage steps applied to one cell of a pair. In all cases, cell pairs were superfused with 1 mM halothane to reduce g_j and record single channel current events. These events were digitized at 1 kHz and plotted at 500 Hz. Event histograms during long current recordings were performed by measuring only transitions >200 ms between conductive states with a digitizing board (Summagraphics; GTCO, Scottsdale, AZ) from currents plotted in chart recorder paper (Windograf 900; Gould Instruments Systems, Valley View, OH). A second method used to determine single channel conductance was the analysis by all-points histograms of the I_j transitions in selected traces. Traces were filtered through an eight-point Bessel low-pass filter (Krohn-Hite, Cambridge, MA). Curve fitting was performed using Origin software (Microcal Software), and Figs. 1–5 were prepared using Adobe Photoshop (Adobe Systems, San Jose, CA). Statistical analysis between the different parameter values was carried out using a Student's *t*-test, where P values <0.05 were considered significant.

RESULTS

Cx36 Is Expressed in Freshly Dispersed β-Cell Pairs

To determine the enrichment of β-cells in our islet cell preparations at the same culture time than that used for electrophysiological recordings, immunocytochemical studies were performed. Most cells in cultures of 8 h were identified as β-cells (90%) using a specific anti-porcine insulin antibody. Specificity of labeling was indicated by the negative staining of fibroblasts found in islet cell cultures grown for 36 h (data not shown) and by the staining of the islets but not of the exocrine cells in pancreatic sections (Fig. 1*C*). To investigate whether Cx36 protein was expressed in freshly dispersed β-cells, double labeling experiments were performed. After their incubation with the anti-insulin antibody, cells were exposed to a specific affinity-purified polyclonal antibody against amino acids of the carboxyl terminus of rat and mouse Cx36. Figure 1 shows that Cx36 was found in most β-cells cultured for 8 h (Fig. 1, *A* and *B*), including cell pairs (Fig. 1, *inset*). Specificity of labeling with the anti-Cx36 antibody was confirmed by staining neuronal cell bodies and projections from the olfactory bulb (Fig. 1*E*) and in vivo islet β-cells (Fig. 1*D*), but not cells from the exocrine pancreas (Fig. 1*D*) used as positive and negative controls (15, 40). To further document that our cell preparation expressed Cx36, total RNA was isolated from freshly isolated islets from adult mice and subjected to RT-PCR using two different intron-spanning combinations of oligonucleotide primers against this connexin. Figure 1, *right*, shows a photograph of a representative gel electrophoresis in which Cx36 expected amplicons of 917 (*a* and *b*) and 447 (*c* and *d*) bp were detected in lanes loaded with RT-PCR products obtained from islets (*a* and *c*) and olfactory bulb (*b* and *d*) RNA. In contrast, no bands were detected in reactions performed in samples in which RT was omitted as well as in

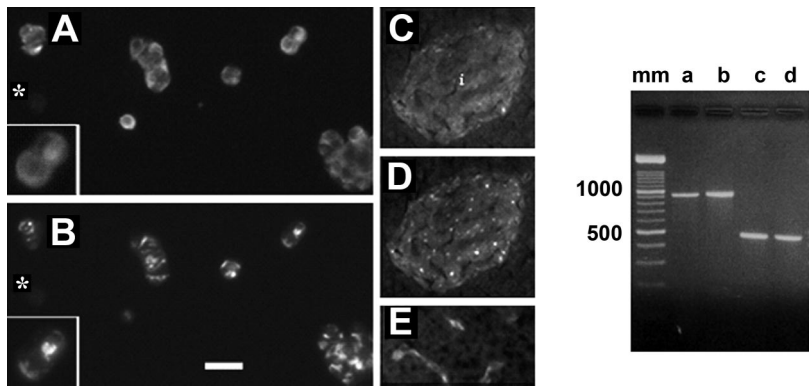

Fig. 1. Identification of connexin (Cx)-36 in freshly dissociated β-cells. *Left*: digitized images of FITC (*A*, *C*, and *E*) and rhodamine (*B* and *D*) fluorescence emitted by dissociated mouse islet cells cultured for 8 h (*A* and *B*) and a pancreatic tissue section (*C* and *D*). Images were obtained after islet cells and pancreatic sections were double labeled with a guinea pig antiserum against porcine insulin (*A* and C) and an affinity-purified polyclonal antibody directed against a peptide of the carboxyl terminus of rat and mouse Cx36 (*B* and *D*). Most freshly dissociated cells, including cell pairs, were identified as β-type (*A*) and express Cx36 (*B*). A negatively labeled cultured cell is indicated (*). *Inset*: amplified images of the cell pair shown in *A* and *B*. Specificity of both antibodies was indicated by insulin and Cx36 staining of the islet (i) but not of exocrine acinar cells (C) in pancreatic tissue sections. Labeling of neurons from the olfactory bulb (*E*) also confirms specificity of anti-Cx36 labeling. *Right*: photograph of a representative electrophoresis gel in which the expected Cx36 amplicons of 917 (*a* and *b*) and 447 bp (*c* and *d*) were detected in lanes loaded with RT-PCR products obtained from islets (*a* and *c*) and olfactory bulb (*b* and *d*), but not in control reactions (see text). mm, Molecular ladder. Calibration bars: *A* and *B* = 30 μm; *insets* = 15 μm; *C–E* = 50 μm.

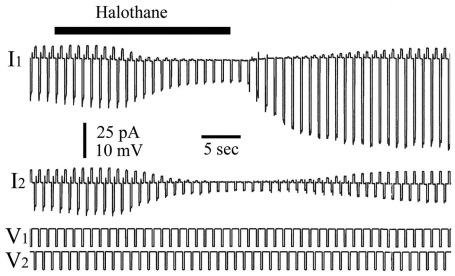

Fig. 2. Halothane reduces junctional currents in mouse β-cell pairs. Membrane currents of a dual whole cell voltage-clamp pair of freshly dispersed mouse β-cells. Currents were recorded during the application of a voltage pulse protocol shown at *bottom*. The junctional currents correspond to the upward transitions in each trace. In control conditions, junctional current transitions remained constant, but they were reduced during the application of halothane. After halothane washout (1 min), junctional currents were again recorded, indicating a reversible process of uncoupling.

ones in which RNA was replaced by water (data not shown). Thus we conclude that freshly dispersed β-cell pairs express Cx36.

Junctional Currents Between β-Cells Are Sensitive to Halothane

Consistent with our previous findings (35), a high incidence of electrical coupling was found in dual voltage-clamp whole cell pairs (80% = 20 cell pairs); cell mean input resistance was 4.2 ± 0.8 GΩ and the mean g_j was 355 ± 45 pS (n = 20 cell pairs). Results from our previous study (35) where octanol was used as the uncoupling agent suggested that either the γ_j between β-cell pairs was <20 pS or their openings and closings were distinct from other gap junction channels characterized at that time (see above). To discern between these possibilities, we improved our signal-to-noise ratio by a factor of four by reducing activity of most membrane channels using specific pipette and external solutions (see METHODS) and using halothane as the uncoupling agent. Halothane has been found to increase the closing time but not the unitary conductance of many gap junction channels (8). The effect of this drug on g_j from β-cell pairs had not been tested before. Figure 2 shows representative I_j and I_{nj} currents from one of the seven β-cell pairs exposed to halothane. Cells were maintained at a holding potential of 0 mV during the application of the slow-frequency pulse protocol (see METHODS). Few seconds after adding 1 mM halothane to the bath-superfusing solution, a transient small increase in I_j and I_{nj} was recorded in both cells from the pair that mainly result from a transient increase in I_j. This change was followed by a large reduction in I_j that rapidly approached zero. This latter effect, known as gap junction chemical gating, was fully reversible after the anesthetic was washed out, demonstrating that gap junction channels between these cells are sensitive to halothane.

β-Cells Communicate through Gap Junction Channels with a Very Small Unitary Conductance

During cycles of uncoupling induced by 1 mM halothane, very small current transitions between conductive states or between conductive and nonconductive states were recorded in I_j despite membrane electrical noise. These transitions demonstrate that gap junction channels electrically communicate freshly isolated mouse β-cell pairs. Figure 3*A* shows I_j and I_{nj} traces from one cell pair where transitions of the same duration and opposite polarity were recorded during the application of a junctional voltage (V_j) of 50 mV. Noise resolution level in I_j was 0.2 pA. On top of the I_j traces, an expanded segment is shown. The unitary g_j was calculated using two methods. In the first method, multiple current transitions were measured, and all events were pooled into histograms where the mean ± SE

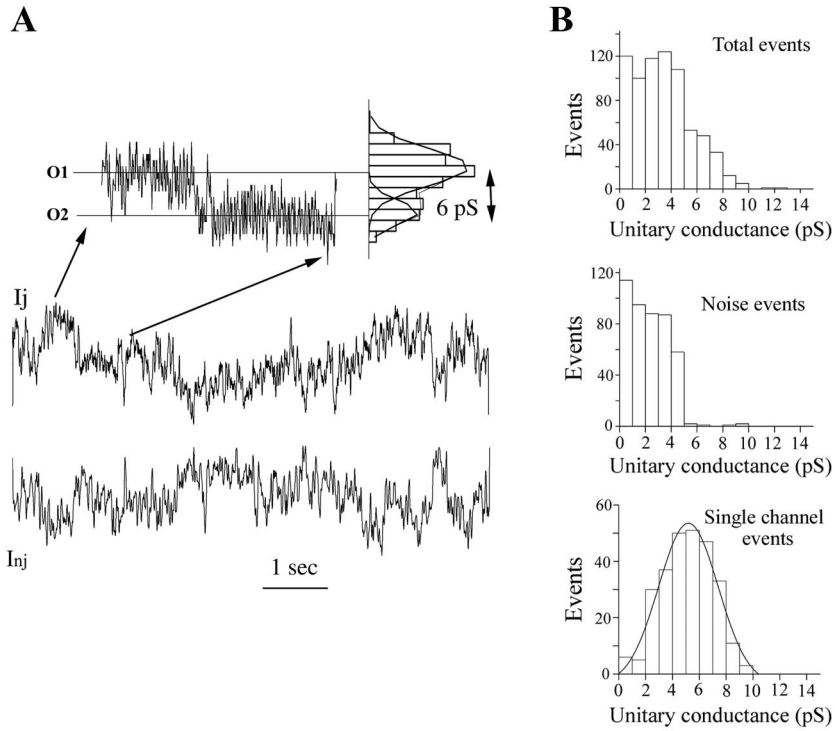

Fig. 3. Unitary current transitions between freshly dispersed mouse β-cell pairs yield small conductances. *A*: current recordings from a cell pair under a dual whole cell voltage clamp indicating small unitary transitions. The I_j and nonjunctional currents (I_{nj}) are presented to show that the small transitions are undoubtedly gap junction channels. Selected regions where junctional transitions are unambiguous, indicated by arrows, were expanded at the *top* to determine unitary conductance. The all-points histogram at *right* of the expanded current trace indicates that the differences between conductive states represent a junctional conductance (g_j) of 6 pS. Noise resolution level in I_j was 0.2 pA. *B*: frequency histograms of pooled events. *Top*, all transitions recorded from three different cell pairs, measured from 90 s of recordings of transjunctional currents obtained during halothane application. *Middle*, events accumulated from five different cell pairs obtained when a voltage pulse was applied to one cell but no g_j was detected. *Bottom*, distribution of junctional current events obtained after subtracting all transitions recorded from the noise-associated events.

was determined as shown in Fig. 3*B*. Figure 3*B*, *top*, represents all the events measured from I_j traces recorded from three distinct β-cell pairs while junctional channels were active during the application of a transjunctional voltage pulse of 50 mV. The bin width was selected as 1 pA, which is half the detection threshold resolution. A main peak was detected at 3.9 ± 0.8 pS. Because of the reduced size of these currents, to eliminate those events that corresponded to nonjunctional membrane, an equal number of transitions was measured from four cell pairs where I_j was not detected during the application of a transjunctional voltage of 50 mV. The corresponding histogram is shown in Fig. 3*B*, *middle*. The subtraction between total and nonjunctional histogram events is shown in Fig. 3*B*, *bottom*, and yielded a γ_j of 5.1 ± 0.7 pS. In the second method, transjunctional current levels were digitized point by point, and an all-points histogram was calculated. An example of the latter is shown (Fig. 3*A*) at the right of the I_j expanded trace, where a γ_j of 6 pS was calculated by subtracting the mean of Gaussian distributions for each level. This value is not significantly different from the one obtained using the digitizing method.

Gap Junctions from β-Cells Exhibited Weak Voltage Dependence

In the past years, it has been shown that gap junction channels formed by almost all connexins have specific voltage sensitivity (6). Thus transjunctional voltage sensitivity is a property that helps identify the connexin isotype present in a junction. In a previous study, we had not detected transjunctional voltage dependence in g_j recordings from isolated β-cell pairs (35). However, it is possible that this nondetection resulted from the fast voltage/time rate of change of the applied ramps (18 mV/s), which may have masked a slow voltage dependence (see DISCUSSION). Therefore, in our present study, we applied slow voltage ramps (1–2 mV/s) during 50 or 100 s to one cell of the pair. In four out of seven cell pairs where sustained high-input membrane resistance in both cells allowed its study (mean = 4.2 GΩ), the relationship between I_j and V_j was linear from −100 to 100 mV, indicating a lack of transjunctional voltage sensitivity. However, in three cell pairs, junctional channels showed a clear, although weak, voltage dependence. As shown in Fig. 4*A*, the transjunctional currents for one of these cells increased monotonically during the first part of the positive or negative ramps, but, after 30 s when transjunctional voltages reached ~60 mV, the current decreased, approaching its minimum at 90–100 mV. The nonlinearity of the I_j-V_j relation indicates the presence of voltage-gated gap junction channels. Dividing the current traces shown in Fig. 4*A* by the applied voltage ramp, we obtained the g_j along the ramp protocols. In Fig. 4*B*, we present the G_j (normalized g_j) and V_j relation from the cell pair shown above. Because of the low signal-to-noise ratio, a robust dispersion of points for G_j values was obtained for values close to 0 mV. The digitized G_j values became smaller as the voltage increased. The best fit for this change in conductance corresponds to a two-state Boltzmann relation with the following parameters: G_{max} = 1.0, G_{min} = 0.3 and 0.28, A = 0.21 and 0.23, and V_o = −85 and 87 mV for positive and negative voltage pulses, respectively.

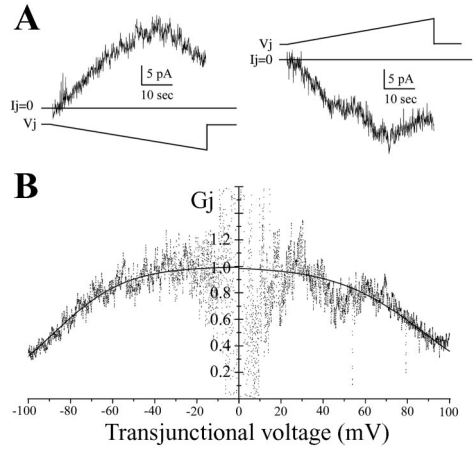

Fig. 4. Voltage gating of junctional channels between freshly isolated β-cell pairs. *A*: transjunctional currents obtained during the application of a hyperpolarizing (*left*) or depolarizing (*right*) voltage ramp to the contiguous cell. Note that the increment at low potential is linear for the first part, but, beyond ±50–60 mV, the current becomes smaller. *B*: all points represent the normalized G_j calculated from the curves shown in *A* that were obtained after dividing the digitized junctional current-time curve by the transjunctional voltage ramp applied at both polarities from 0 to ±100 mV. The initial potential for both cells was 0 mV. The continuous line at each curve indicates the best fit for a Boltzmann relation. Each half was adjusted independently.

Junctional Currents in Freshly Dispersed β-Cell Pairs Are Insensitive to Quinine

Using deficiently coupled cells transfected with specific connexins, it has been found that quinine selectively uncouples gap junctions formed of Cx36 and Cx50 but not those formed of Cx26, Cx32, Cx43, or Cx40 (43). When a β-cell pair was exposed for several minutes to 1 mM quinine, no changes in g_j recordings were detected (Fig. 5*C*). Thereafter, g_j was decreased by adding 2 mM halothane to the bath solution (data not shown). Similar results were found in five other cell pairs. As a positive control, we tested for quinine effects on g_j of N2A cells transfected with Cx50. In Fig. 5*A*, we show a g_j recording at the single channel level where Cx50 channels are actively opening and closing at a transjunctional potential of 30 mV. Note that two open states are present with an estimated conductance of 210 pS. Figure 5*B* shows that 1 mM quinine rapidly reduces the activity of Cx50 channels. These results strongly suggest that gap junction channels in β-cells are insensitive to 1 mM quinine.

DISCUSSION

Previous characterization of microscopic properties of g_j in dual voltage-clamp isolated mouse β-cell pairs was prevented by a relative low signal-to-noise ratio (20 pS) resolution (35). In the present work, high-resolution signal-to-noise ratio recordings (5 pS) allow us to show for the first time the gap junction unitary conductance recorded from pancreatic β-cells.

Unitary Conductance

Halothane uncoupling effects on g_j in β-cells have not been previously reported. Halothane completely suppressed g_j. Before reaching g_j = 0, we detected very small transitions between two different conductive states. According to data presented for other connexins, we presume that the γ_j calcu-

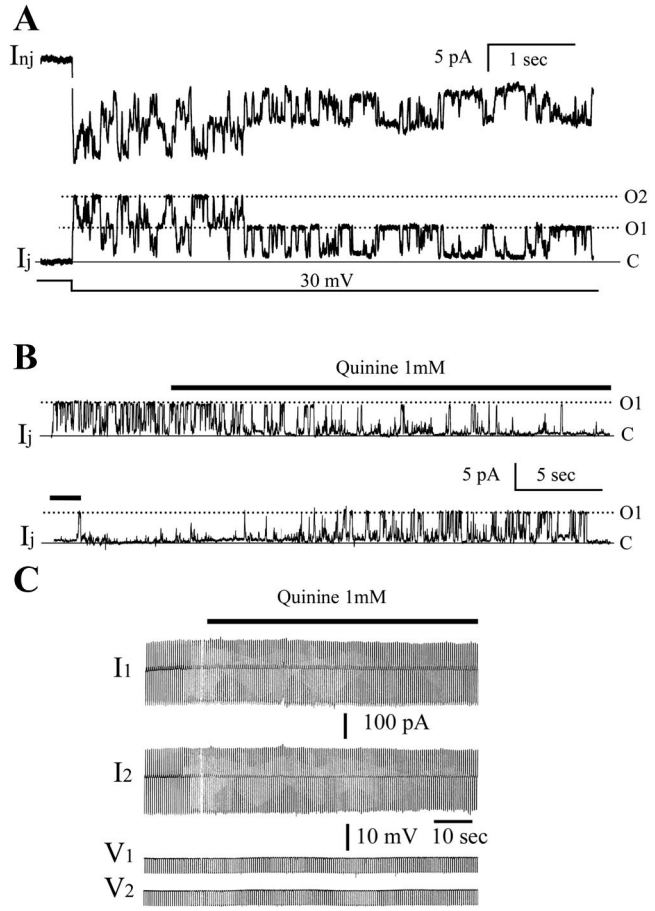

Fig. 5. Quinine uncouples N2A cells expressing Cx50 but does not reduce junctional currents between freshly isolated β-cell pairs. *A*: membrane currents from a dual voltage-clamped isolated pair of N2A cells transfected with Cx50 recorded during the application of a sustained hyperpolarizing voltage step (−30 mV) shown at *bottom*. Two unitary current levels are clearly observed at the beginning of the pulse (O1 and O2). Currents were filtered at 600 Hz. *B*: during the application of 1 mM quinine (black line), unitary junctional currents rapidly decreased. Currents were filtered at 200 Hz. In contrast, junctional currents between isolated β-cell pairs (C) were similar before and 5 min after application of 1 mM quinine to the bath solution.

lated for these transitions corresponds to the main unitary conductance of the channels, since chemical gating facilitates transitions from the main to the closed state (7). Although transjunctional voltage has been shown to facilitate the transitions from the main γ_j to the residual state (29, 34, 51), we do not expect to observe a substantial number of V_j-dependent transitions, since our recordings were performed at ±50 mV, a value much lower than their calculated V_o (see below). After application of 1 mM halothane, we were able to calculate a γ_j from 5 to 10 pS (mean of 5.1 pS). This value is similar, although within the lower range, to the ones reported for the main γ_j in N2A (44) and HeLa (46) cells transfected with Cx36. This similarity supports the idea that functional gap junction channels in β-cells are mainly formed with Cx36. This γ_j is within the smallest range reported for any other gap junction channel. Considering a V_o of ±85 mV, the open probability of gap junction channel recordings at V_j of ±50 mV should be around its maximum. From the mean g_j and γ_j reported here, it is expected that ~60 gap junction channels interconnected isolated β-cell pairs. This estimated number is consistent with the few particles and small size of gap junctions described in islet cells by cryofracture and electron microscopic studies (17, 25). It is also consistent with the value of junctional resistance calculated from intracellular membrane potential recordings obtained from pairs of β-cells within a microdissected islet (11).

Voltage Dependence

The present study also provides evidence for a weak voltage dependence in three out of seven freshly isolated β-cell pairs where high membrane input conductance allowed its study with a slow ramp protocol (1–2 mV/s: 50–100 s). We have found that the gating by transjunctional voltage of β-cell gap junction channels is quite restricted to values larger than ±60 mV with a V_o close to ±85 mV. This V_o value is similar to the one found for Cx36 channels recorded in expression cell systems (1, 44, 46), which is one of the connexins less sensitive to voltage so far characterized. Thus functional properties of β-cell gap junction channels reported here (Fig. 1) are consistent with molecular data previously reported (20, 40; shown here also), which indicates that Cx36 is a major molecular component of their gap junctions. Nonetheless, not all cell pairs rendered the same voltage sensitivity. In four out of seven cell pairs, g_j was not significantly voltage dependent. It is unlikely that differences in voltage dependence resulted from recordings of cell pairs from distinct endocrine cell types, considering that cell preparations were highly enriched in β-cells (~90%) and that G_j-V_j recordings were symmetric. A possible factor that may have interfered with the detection of voltage sensitivity is the high series resistance associated with the recording electrodes (49); nonetheless, this is unlikely, since patch micropipettes with resistances not larger than 5 MΩ were used, electrode series resistance was electronically compensated (HEKA), and the mean g_j values from cell pairs recorded was ~350 pS independently of their sensitivity to voltage. Finally, in the present study, it is also unlikely that a slow voltage dependence was kinetically missed, since the voltage ramp protocol applied was slower than the time constant of g_j inactivation already described for Cx36 channels (1, 44, 46). Thus differences in G_j voltage sensitivity suggest that there is heterogeneity in the molecular composition of gap junction channels expressed between β-cells (see below).

Glucose (11–22 mM) induces in β-cells a pattern of electrical activity constituted by a slow and a fast component. The slow component is formed by regular membrane potential oscillations from a silent (−55 mV) to an active (−45 mV) phase. The fast component involves bursts of voltage-dependent Ca^{2+} and K^+ spikes generated during the active phase. Spike amplitude (30–10 mV) decreases along the active phase, and the membrane potential does not surpass 0 mV (2, 3, 4). Although voltage changes induced by glucose are very dynamic, it is not expected that they modulate g_j in β-cells. Slow oscillations of membrane potential are known to occur synchronous and in phase in most cells within microdissected (26) and in vivo (13) islets. The synchronous shift in voltage from the silent to the active phase (~10–12 mV) of β-cells within an islet will not affect their electrical coupling, since their gap junction channels do not show membrane potential voltage dependence, as we have previously demonstrated (35). Transient transjunctional voltages are expected to occur between

β-cells because of desynchronization of their burst of spikes, particularly during the second half of the active phase (26). However, their expected amplitude is low (voltage = 30–10 mV, see above) compared with the large V_o ±85 mV reported here for β-cell pair gap junction channels. Therefore, the effect of transjunctional voltage on g_j is expected to be negligible.

Sensitivity to Quinine

The low γ_j and the weak voltage dependence reported here in isolated pairs of β-cells suggested that Cx36 is intercommunicating these cells, and this prompted us to test for quinine effects on g_j. According to our data, g_j between β-cells is not sensitive to quinine at doses of 1 mM in cell pairs where chemical gating was readily induced by 1 mM halothane. Uncoupling of N2A Cx50 transfected cells (Fig. 5) demonstrates that 1 mM quinine was effective to reduce the g_j of junctions formed by channels sensitive to this drug. Lower concentrations of quinine have been found to be required to uncouple Cx50 (EC_{50} = 75 μM), and even lesser ones were required to close Cx36 (EC_{50} = 35 μM) gap junction channels expressed in mammalian cell lines (43). Thus the lack of sensitivity of g_j to quinine also suggests a molecular difference between β-cell and Cx36 gap junction channels.

Biophysical Properties of Gap Junction Channels Recorded in β-Cells Are Similar Although Not Identical to Those Described for Cx36 Channels

The data presented here show that some gap junction channels in β-cells had very similar γ_j and V_o to those described for Cx36 channels in mammalian expression cell systems. However, g_j recordings in some cell pairs showed no voltage dependence. Moreover, g_j in all cell pairs recorded was insensitive to quinine, indicating that the properties of their gap junction channels do not exactly replicate those of Cx36. These findings suggest that the gap junctions in β-cells are not molecularly identical to Cx36. The following three cell mechanisms may account for these differences.

The first is expression of distinct transcripts of Cx36 in different mammalian cell types. Although it has not yet been described for any of the cells known to express Cx36, it is possible, since the Cx36 coding sequence is contained in two exons separated by an intron (52). β-Cell g_j insensitivity to quinine may result by this cell mechanism. However, heterogeneity in the V_j-G_j was recorded. Thus, if β-cells express only one connexin, the expression of two distinct Cx36 transcripts in β-cells should be considered. To our knowledge, the expression of more than one connexin or protein transcript subtype in a single cell type has not been documented, making this cell mechanism a less probable one.

Second, differential posttranslational modification of Cx36 in some β-cell pairs may also explain differences. Connexins are known to be phosphoproteins (19), and phosphorylation is known to modify γ_j of gap junction channels (18, 30). Although in bovine retina Cx36 has not been found to be phosphorylated (41), it is known that connexin phosphorylation is cell and species specific (18). In addition, hemichannel activity of perch Cx35, which is an ortholog of Cx36, is reduced by an analog of cAMP. The phosphorylation consensus sequence responsible for this modulation is also present in Cx36 (27). A differential degree of Cx36 phosphorylation, depending on β-cell localization within an islet, may occur in vivo. Peripheral β-cells are more exposed to paracrine stimulation induced by molecules released by other endocrine cell types than the inner localized ones (see Introduction), which may allow for V_j-G_j heterogeneity. Finally, interaction of Cx36 with other possible connexins expressed in β-cells (see below) may induce the appearance of phosphorylated forms with slower electrophoretic mobilities, since it occurs with Cx43 when combined with Cx45 (53)

A third possible mechanism that may account for differences found between N2A Cx36 and β-cell channels is the expression of heteromeric channels formed with Cx36 and other connexins possibly expressed by β-cells. Most cells studied up to now express more than one connexin. In homomeric gap junction channels, connexins are formed by only one connexin isotype (30, 51), whereas, in heterotypic channels, each connexin is formed by a different connexin isotype as shown by recordings of g_j from isolated pairs of amphibian and mammalian cell systems where controlled expression of specific connexins was performed (28, 45). In addition, different connexin isotypes expressed in the same cell are capable of forming heteromeric connexins with specific permeability to fluorescent molecules and varied responses to second messengers, as indicated by experiments of coimmunoprecipitation (5, 21). Further evidence for the presence of heteromeric intercellular channels and for the demonstration that their gating properties depend on their specific connexin molecular composition came from recordings from native cells that express more than one connexin subtype (12). Considerable effort has been made to molecularly identify connexins expressed in β-cells (see Introduction). However, because of the small size of β-cell gap junctions (17, 25) and the large number of gap junction proteins cloned, whether Cx36 is coexpressed with other connexin(s) is still an open question (see Introduction). The heterogeneity in the G_j-V_j here reported in β-cells is a sensitive parameter that provides evidence to support this latter possibility. As mentioned before (see Introduction), experiments using islets from different types of mice with connexins embedded with LacZ reporter genes have not ruled out the possibility that Cx43, Cx45, or both connexins are expressed in β-cells (47). By comparing V_o and γ_j obtained from our g_j recordings, we excluded the possibility that Cx43 or Cx45 formed homomeric channels in gap junctions between isolated β-cell pairs. However, our data do not exclude the possibility that these connexins might be coexpressed in a heteromeric configuration with Cx36. Besides them, other gap junction proteins from the ones already investigated may be coexpressed with Cx36 in β-cells. In any case, the steady-state G_j-V_j relationship was symmetrical independently that junctions between β-cell pairs exhibited or not voltage dependence. Thus, if another connexin is expressed in β-cells, it likely oligomerizes with Cx36 in a heteromeric configuration.

The consequences of heteromeric connexin formation on biophysical properties of gap junction channels are only beginning to emerge. With regard to γ_j in mammalian systems where Cx45 and Cx43 (53), or Cx43 and Cx40 (10), have been coexpressed, it has been observed that the resulting heteromeric channels exhibit reduced unitary conductances. Few data are available addressing the impact of heteromeric channel formation on voltage dependence (10) and drug sensitivity properties (21). Nonetheless, evidence exists that formation of

heteromeric combinations changes the gating properties induced by voltage (53), pH (14), and phosphorylation (21). Taking this into account, β-cells might express heteromeric connexins made of Cx36 and other connexin(s), and this may be contributing to the weaker and heterogeneous transjunctional voltage dependence of their g_j recordings compared with that recorded for homomeric Cx36 channels in expression cell systems. Heteromeric channel formation may also explain differences in quinine sensitivity.

In summary, although the electrophysiological data presented here are consistent with the notion that Cx36 is a major molecular component of functional gap junction channels in freshly isolated mouse β-cells, their channel properties are not identical to those observed for this connexin expressed in mammalian cell systems. The cellular mechanism(s) underlying these differences remains to be investigated. Overall, unambiguous recordings of unitary gap junction currents presented here might have significant implications in the understanding of the physiological role of gap junctions in β-cell function.

ACKNOWLEDGMENTS

We thank Patricia Mantel, Lourdes Cruz-Miguel, and Felix Paisano for excellent technical support during this study.

GRANTS

The International Women Cooperation Program, funded by the National Science Foundation and the American Association for the Advancement of Science, awarded E. M. Pérez-Armendariz and A. P. Moreno with Grant No. INT0003057 that provided the funds to start and develop in part this project. This work was also funded by Consejo Nacional de Ciencia y Tecnología-México Grant No. D42044-M, a Universidad Nacional Autónoma de México-México Travel Grant, and National Heart, Lung, and Blood Institute Grant R01 HL-63969–05.

REFERENCES

1. **Al-Ubaidi MR, White TW, Ripps H, Poras I, Avner P, Gomes D, and Bruzzone R.** Functional properties, developmental regulation, and chromosomal localization of murine connexin36, a gap-junctional protein expressed preferentially in retina and brain. *J Neurosci Res* 59: 813–826, 2000.
2. **Ashcroft FM and Rorsman P.** Electrophysiology of the pancreatic beta-cell. *Prog Biophys Mol Biol* 54: 87–143, 1989.
3. **Atwater I, Dawson CM, Scott A, Eddlestone G, and Rojas E.** The nature of the oscillatory behaviour in electrical activity from pancreatic beta-cell. *Horm Metab Res Suppl* 10: 100–107, 1980.
4. **Atwater I, Kukuljan M, and Pérez-Armendariz EM.** Molecular biology of the ion channels in the pancreatic B-cell. In: *Molecular Biology of Diabetes,* edited by Draznin B and LeRoith D. Tototwa, NJ: Humana, 1994, p. 303–332.
5. **Bevans CG, Kordel M, Rhee SK, and Harris AL.** Isoform composition of connexin channels determines selectivity among second messengers and uncharged molecules. *J Biol Chem* 273: 2808–2816, 1998.
6. **Bruzzone R, White TW, and Paul DL.** Connections with connexins: the molecular basis of direct intercellular signaling. *Eur J Biochem* 238: 1–27, 1996.
7. **Bukauskas FF and Peracchia C.** Two distinct gating mechanisms in gap junction channels: CO2-sensitive and voltage-sensitive. *Biophys J* 72: 2137–2142, 1997.
8. **Burt JM and Spray DC.** Volatile anesthetics block intercellular communication between neonatal rat myocardial cells. *Circ Res* 65: 829–837, 1989.
9. **Charollais A, Serre V, Mock C, Cogne F, Bosco D, and Meda P.** Loss of alpha 1 connexin does not alter the prenatal differentiation of pancreatic beta cells and leads to the identification of another islet cell connexin. *Dev Genet* 24: 13–26, 1999.
10. **Cottrell GT, Wu Y, and Burt JM.** Cx40 and Cx43 expression ratio influences heteromeric/ heterotypic gap junction channel properties. *Am J Physiol Cell Physiol* 282: C1469–C1482, 2002.
11. **Eddlestone GT, Goncalves A, Bangham JA, and Rojas E.** Electrical coupling between cells in islets of Langerhans from mouse. *J Membr Biol* 77: 1–14, 1984.
12. **Elenes S, Rubart M, and Moreno AP.** Junctional communication between isolated pairs of canine atrial cells is mediated by homogeneous and heterogeneous gap junction channels. *J Cardiovasc Electrophysiol* 10: 990–1004, 1999.
13. **Gomis A, Sanchez-Andres JV, and Valdeolmillos M.** Oscillatory patterns of electrical activity in mouse pancreatic islets of Langerhans recorded in vivo. *Pflügers Arch* 432: 510–515, 1996.
14. **Gu H, Ek-Vitorin JF, Taffet SM, and Delmar M.** Coexpression of connexins 40 and 43 enhances the pH sensitivity of gap junctions: a model for synergistic interactions among connexins. *Circ Res* 86: E98–E103, 2000.
15. **Guldenagel M, Ammermuller J, Feigenspan A, Teubner B, Degen J, Sohl G, Willecke K, and Weiler R.** Visual transmission deficits in mice with targeted disruption of the gap junction gene connexin36. *J Neurosci* 21: 6036–6044, 2001.
16. **Harris AL.** Voltage-sensing and substate rectification: moving parts of connexin channels. *J Gen Physiol* 119: 165–169, 2002.
17. **In't Veld PA, Pipeleers DG, and Gepts W.** Glucose alters configuration of gap junctions between pancreatic islet cells. *Am J Physiol Cell Physiol* 251: C191–C196, 1986.
18. **Kwak BR, Saez JC, Wilders R, Chanson M, Fishman GI, Hertzberg EL, Spray DC, and Jongsma HJ.** Effects of cGMP-dependent phosphorylation on rat and human connexin43 gap junction channels. *Pflügers Arch* 430: 770–778, 1995.
19. **Lampe PD and Lau AF.** The effects of connexin phosphorylation on gap junctional communication. *Int J Biochem Cell Biol* 36: 1171–1186, 2004.
20. **Le Gurun S, Martin D, Formenton A, Maechler P, Caille D, Waeber G, Meda P, and Haefliger JA.** Connexin-36 contributes to control function of insulin-producing cells.. *J Biol Chem* 278: 37690–37697, 2003.
21. **Martinez AD, Hayrapetyan V, Moreno AP, and Beyer EC.** Connexin43 and connexin45 form heteromeric gap junction channels in which individual components determine permeability and regulation. *Circ Res* 90: 1100–1107, 2002.
22. **Meda P.** Cx36 involvement in insulin secretion: characteristics and mechanism. *Cell Commun Adhes* 10: 431–435, 2003.
23. **Meda P, Chanson M, Pepper M, Giordano E, Bosco D, Traub O, Willecke K, el Aoumari A, Gros D, Beyer EC, Orci L, and Spray DC.** In vivo modulation of connexin 43 gene expression and junctional coupling of pancreatic B-cells. *Exp Cell Res* 192: 469–480, 1991.
24. **Meda P, Pepper MS, Traub O, Willecke K, Gros D, Beyer E, Nicholson B, Paul D, and Orci L.** Differential expression of gap junction connexins in endocrine and exocrine glands. *Endocrinology* 133: 2371–2378, 1993.
25. **Meda P, Perrelet A, and Orci L.** Increase of gap junctions between pancreatic B-cells during stimulation of insulin secretion. *J Cell Biol* 82: 441–448, 1979.
26. **Meissner HP.** Electrophysiological evidence for coupling between beta cells of pancreatic islets. *Nature* 262: 502–504, 1976.
27. **Mitropoulou G and Bruzzone R.** Modulation of perch connexin35 hemi-channels by cyclic AMP requires a protein kinase A phosphorylation site. *J Neurosci Res* 72: 147–157, 2003.
28. **Moreno AP, Laing JG, Beyer EC, and Spray DC.** Properties of gap junction channels formed of connexin 45 endogenously expressed in human hepatoma (SKHep1) cells. *Am J Physiol Cell Physiol* 268: C356–C365, 1995.
29. **Moreno AP, Rook MB, Fishman GI, and Spray DC.** Gap junction channels: distinct voltage-sensitive and -insensitive conductance states. *Biophys J* 67: 113–119, 1994a.
30. **Moreno AP, Saéz JC, Fishman GI, and Spray DC.** Human connexin43 gap junction channels. Regulation of unitary conductances by phosphorylation. *Circ Res* 74: 1050–1057, 1994b.
31. **Pérez-Armendariz EM and Atwater I.** Glucose-evoked changes in $[K^+]$ and $[Ca^{2+}]$ in the intercellular spaces of the mouse islet of Langerhans. *Adv Exp Med Biol* 211: 31–51, 1986.
32. **Pérez-Armendariz EM, Atwater I, and Bennett MVL.** Mechanism for fast intercellular communication within a single islet of Langerhans. In:

Pacemaker Activity and Intercellular Communication, edited by Huizinga JD. Boca Raton, FL: CRC, 1995, p. 305–321.

33. **Pérez-Armendariz E, Atwater I, and Rojas E.** Glucose-induced oscillatory changes in extracellular ionized potassium concentration in mouse islets of Langerhans. *Biophys J* 48: 741–749, 1985.
34. **Pérez-Armendariz E, Romano MC, Luna J, Miranda C, Bennett MV, and Moreno AP.** Characterization of gap junctions between pairs of Leydig cells from mouse testis. *Am J Physiol Cell Physiol* 267: C570–C580, 1994.
35. **Pérez-Armendariz M, Roy C, Spray DC, and Bennett MV.** Biophysical properties of gap junctions between freshly dispersed pairs of mouse pancreatic beta cells. *Biophys J* 59: 76–92, 1991.
36. **Pérez-Armendariz EM, Saéz JC, Bravo Moreno JF, Acosta V, Enders G, and Villapando I.** Connexin 43 expression in mouse fetal ovary. *Anat Rec* 271A: 360–367, 2003.
37. **Rash JE, Staines WA, Yasumura T, Patel D, Furman CS, Stelmack GL, and Nagy JI.** Immunogold evidence that neuronal gap junctions in adult rat brain and spinal cord contain connexin-36 but not connexin-32 or connexin-43. *Proc Natl Acad Sci USA* 97: 7573–7578, 2000.
38. **Rosario LM, Atwater I, and Scott AM.** Pulsatil insulin release and electrical activity from single ob/ob mouse islets of Langerhans. *Adv Exp Med Biol* 211: 413–425, 1986.
39. **Santos RM, Rosario LM, Nadal A, García-Sancho J, Soria B, and Valdeolmillos M.** Widespread synchronous [Ca2+]i oscillations due to bursting electrical activity in single pancreatic islets. *Pflügers Arch* 418: 417–422, 1991.
40. **Serre-Beinier V, Le Gurun S, Belluardo N, Trovato-Salinaro A, Charollais A, Haefliger JA, Condorelli DF, and Meda P.** Cx36 preferentially connects β-cells within pancreatic islets. *Diabetes* 49: 727–734, 2000.
41. **Sitaramayya A, Crabb JW, Matesic DF, Margulis A, Singh V, Pulukuri S, and Dang L.** Connexin 36 in *bovine retina*: lack of phosphorylation but evidence for association with phosphorylated proteins. *Vis Neurosci* 20: 385–395, 2003.
42. **Sohl G, Degen J, Teubner B, and Willecke K.** The murine gap junction gene connexin36 is highly expressed in mouse retina and regulated during brain development. *FEBS Lett* 428: 27–31, 1998.
43. **Srinivas M, Hopperstad MG, and Spray DC.** Quinine blocks specific gap junction channel subtypes. *Proc Natl Acad Sci USA* 98: 10942–10947, 2001.
44. **Srinivas M, Rozental R, Kojima T, Dermietzel R, Mehler M, Condorelli DF, Kessler JA, and Spray DC.** Functional properties of channels formed by the neuronal gap junction protein connexin36. *J Neurosci* 19: 9848–9845, 1999.
45. **Steiner E and Ebihara L.** Functional characterization of canine connexin45. *J Membr Biol* 150: 153–161, 1996.
46. **Teubner B, Degen J, Sohl G, Guldenagel M, Bukauskas FF, Trexler EB, Verselis VK, De Zeeuw CI, Lee CG, Kozak CA, Petrasch-Parwez E, Dermietzel R, and Willecke K.** Functional expression of the murine connexin 36 gene coding for a neuron-specific gap junctional protein. *J Membr Biol* 176: 249–262, 2000.
47. **Theis M, Mas C, Doring B, Degen J, Brink C, Caille D, Charollais A, Kruger O, Plum A, Nepote V, Herrera P, Meda P, and Willecke K.** Replacement by a lacZ reporter gene assigns mouse connexin36, 45 and 43 to distinct cell types in pancreatic islets. *Exp Cell Res* 294: 18–29, 2004.
48. **Valiunas V.** Biophysical properties of connexin-45 gap junction hemichannels studied in vertebrate cells. *J Gen Physiol* 119: 147–164, 2002.
49. **Veenstra RD.** Voltage clamp limitations of dual whole-cell gap junction current and voltage recordings. I. Conductance measurements. *Biophys J* 80: 2231–2247, 2001.
50. **Vidaltamayo R, Mery CM, Angeles-Angeles A, Robles-Diaz G, and Hiriart M.** Expression of nerve growth factor in human pancreatic beta cells. *Growth Factors* 21: 103–107, 2003.
51. **Weingart R and Bukauskas FF.** Gap junction channels of insects exhibit a residual conductance. *Pflügers Arch* 424: 192–194, 1993.
52. **Willecke K, Eiberger J, Degen J, Eckardt D, Romualdi A, Guldenagel M, Deutsch U, and Sohl G.** Structural and functional diversity of connexin genes in the mouse and human genome. *Biol Chem* 383: 725–737, 2002.
53. **Zhong G, Hayrapetyan V, and Moreno AP.** The formation of monoheteromeric Cx43-Cx45/Cx45 gap junction channels uncovers gating and selectivity properties of their channels (Abstract). *Biophys J* 82: 633a, 2003.